Lecture 9: Analysis of a paper

- Leuning, R., Cleugh, H.A., Zegelin, S.J. and Hughes, D. (2004).
- Carbon and water fluxes over a temperate *Eucalyptus* forest and a tropical wet/dry savanna in Australia: measurements and comparison with MODIS remote sensing estimates.
- *Agricultural and Forest Meteorology* 129:151-173.

Part 1: Background information

- Study sites
- Climatology
- Data processing
- Quality control

Site locations and local topography

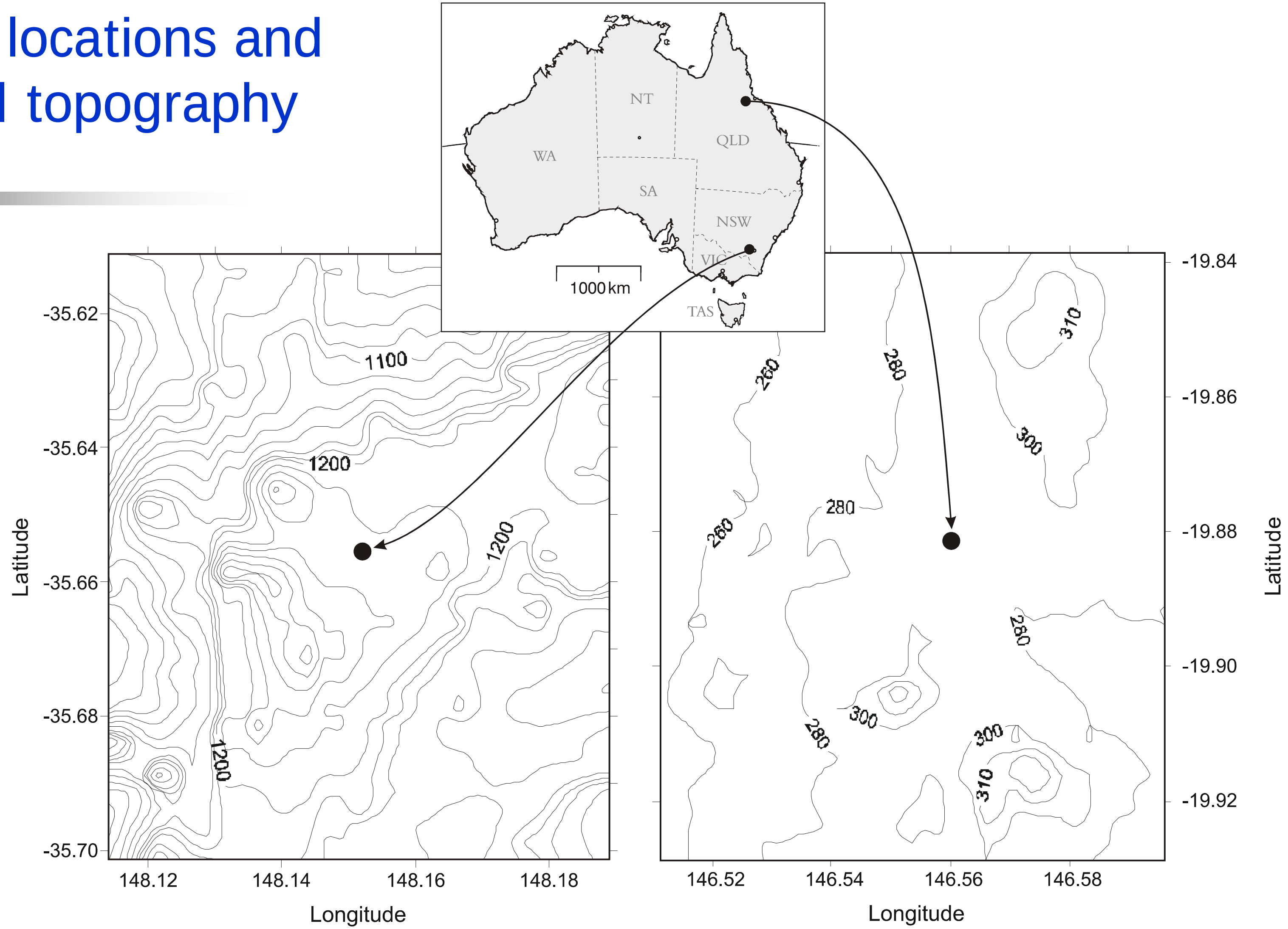

Figure 1. (a) Location within Australia of the two flux stations plus digital elevation maps of the topography at (b) Tumbarumba and (c) Virginia Park and the locations of the flux stations in Australia. The contour interval is 20 m.

Rainfall in measurement years compared to long-term

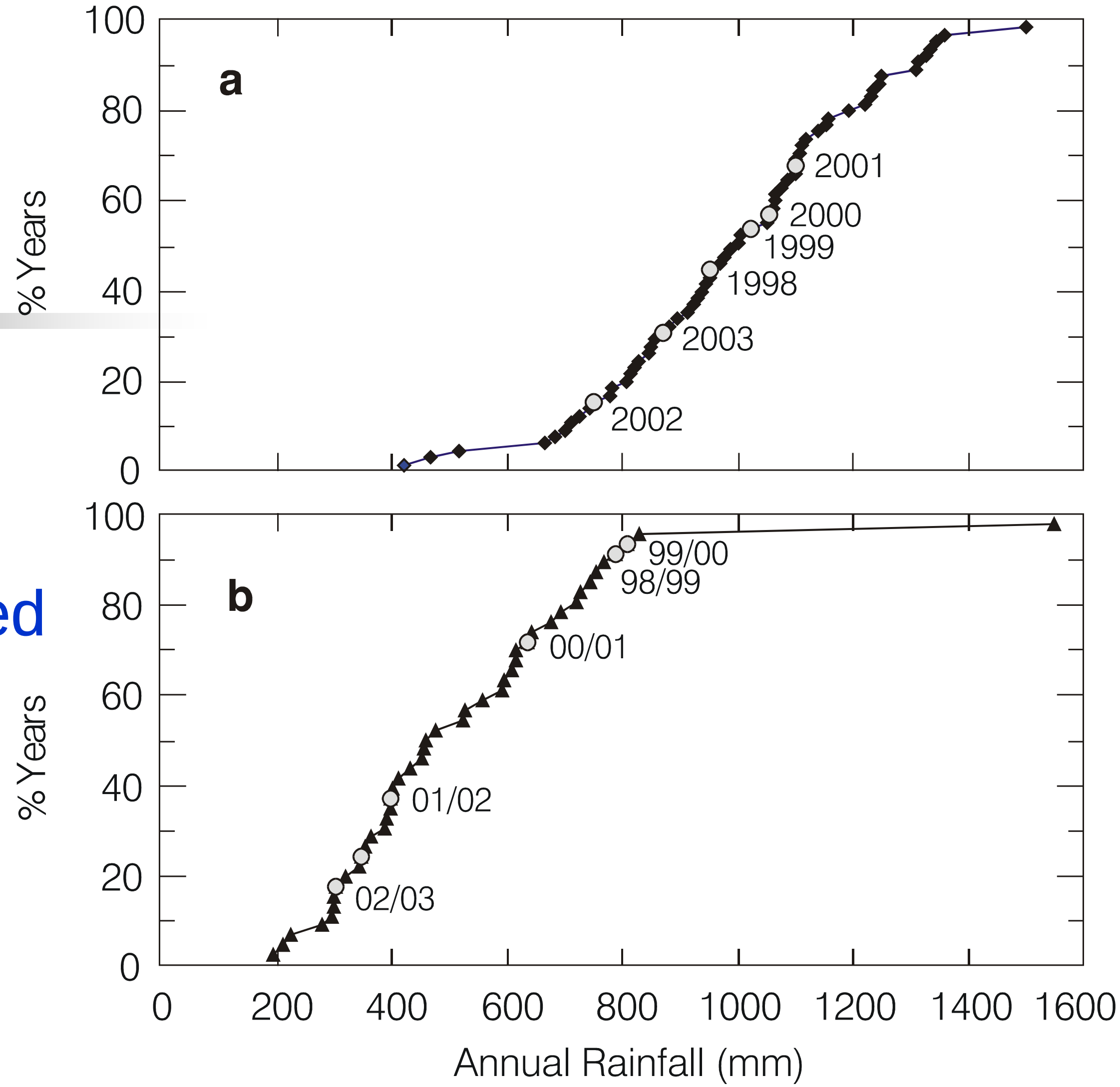

Figure 2. Cumulative probability distributions for rainfall at (a) Tumbarumba Post Office for the period 1940 – 2002, and (b) Charters Towers Post Office for the period 1960 – 2002. The dates shown are for the years during which measurements were made at each flux station.

Rainfall patterns

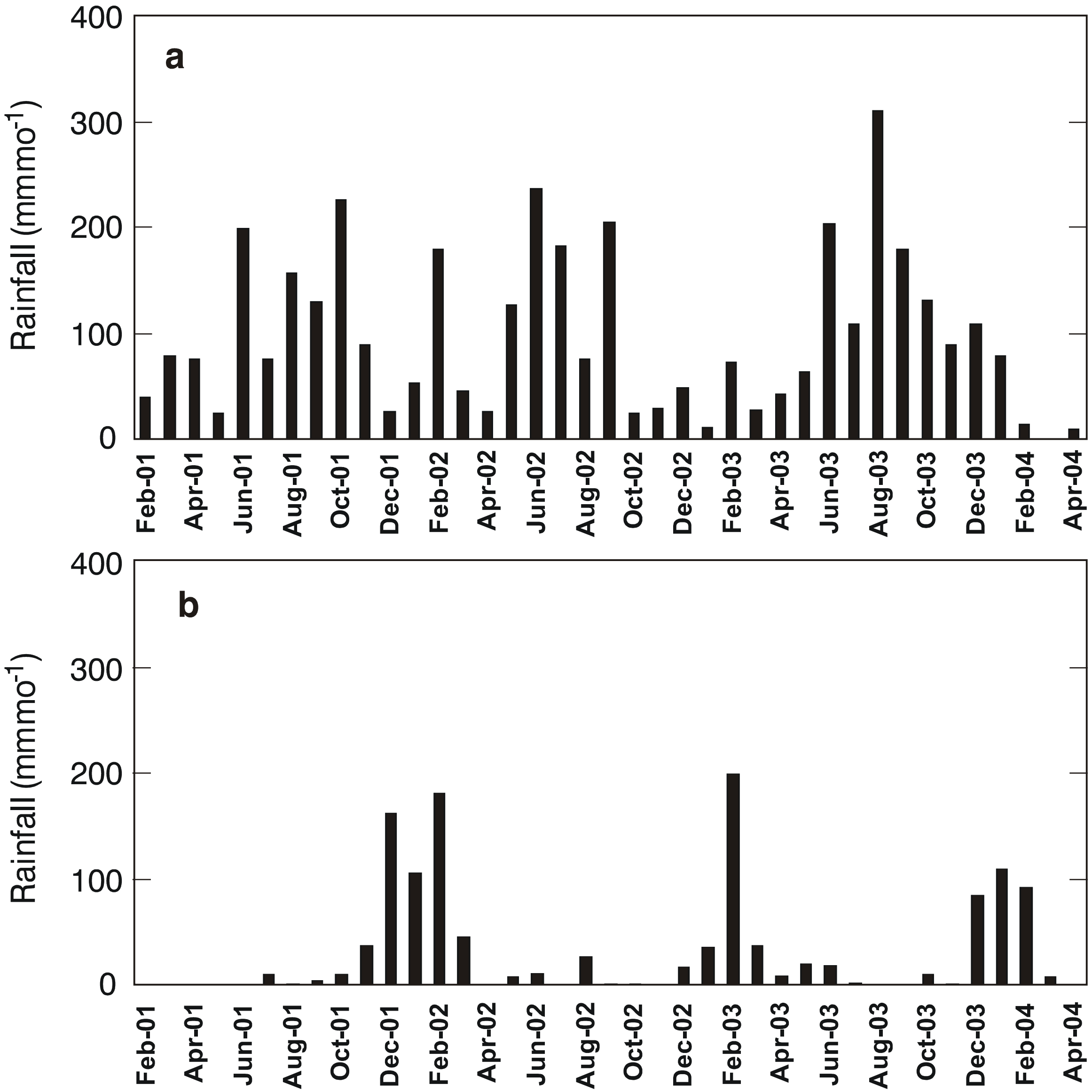

Figure 3. Seasonal rainfall distribution patterns at (a) Tumbarumba and (b) Virginia Park. Rainfall occurs predominantly during the winter months at Tumbarumba and during the summer at Virginia Park.

Neural network analysis for gap filling H and λE

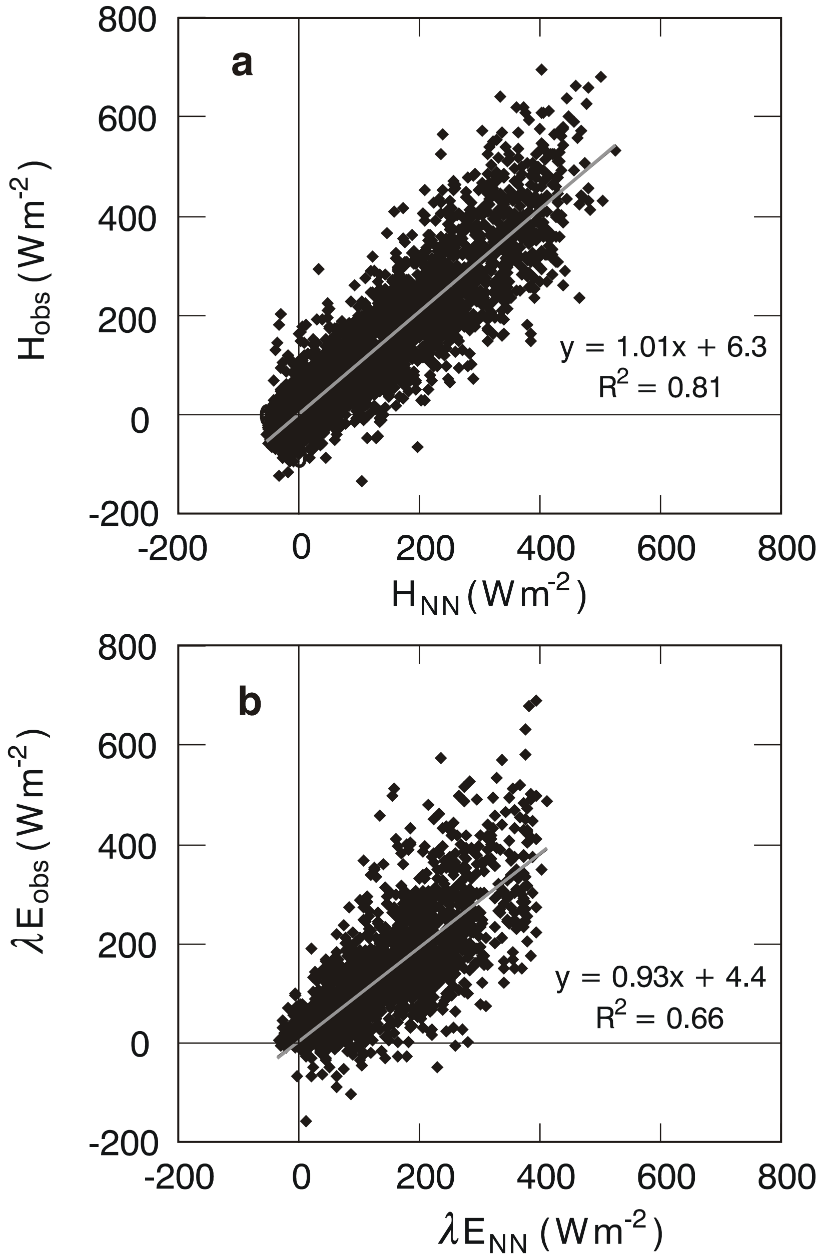

Figure 4. Comparison of observed (a) sensible and (b) latent heat fluxes with corresponding estimates from the neural network analysis.

Neural network analysis for gap filling F_c

Compare with solar radiation

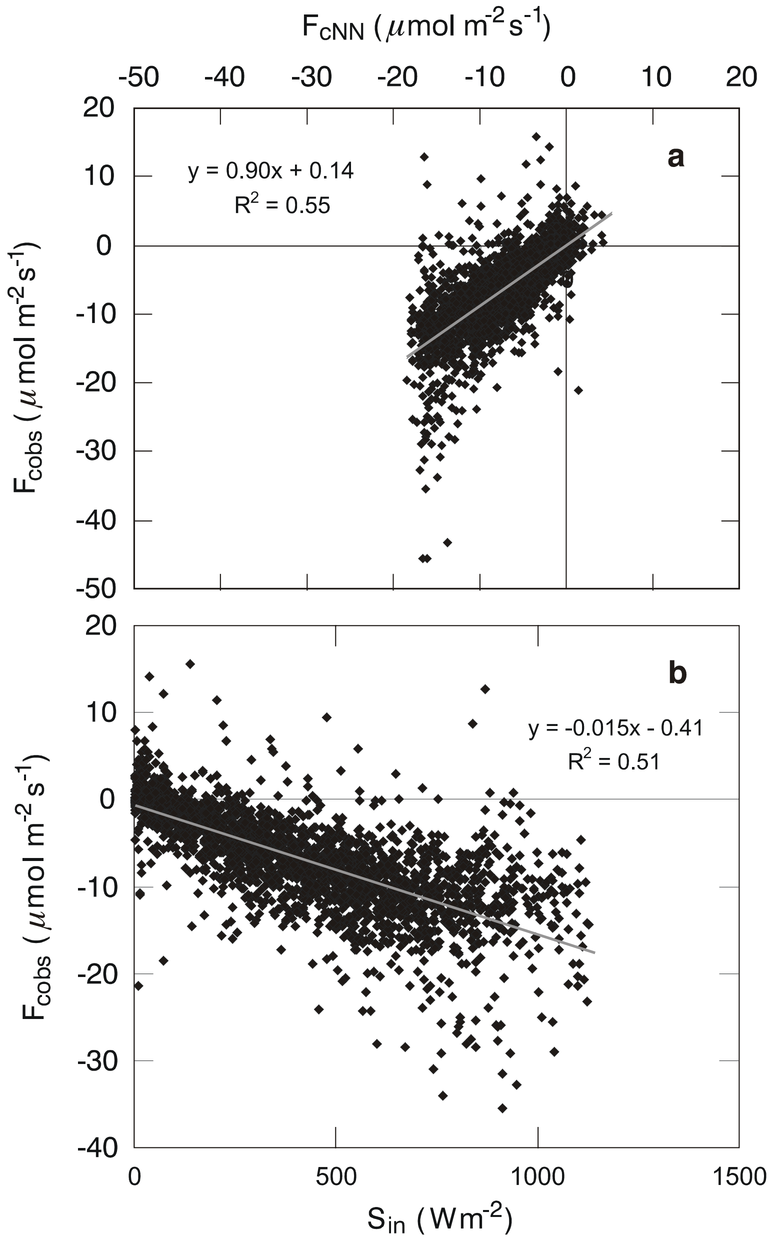

Figure 5. (a) Comparison of observed *Fc* with estimates derived from the neural network analysis, (b) observed *Fc* plotted as a function of incoming solar radiation, *S*in.

Fluxes and concentrations – are they real?

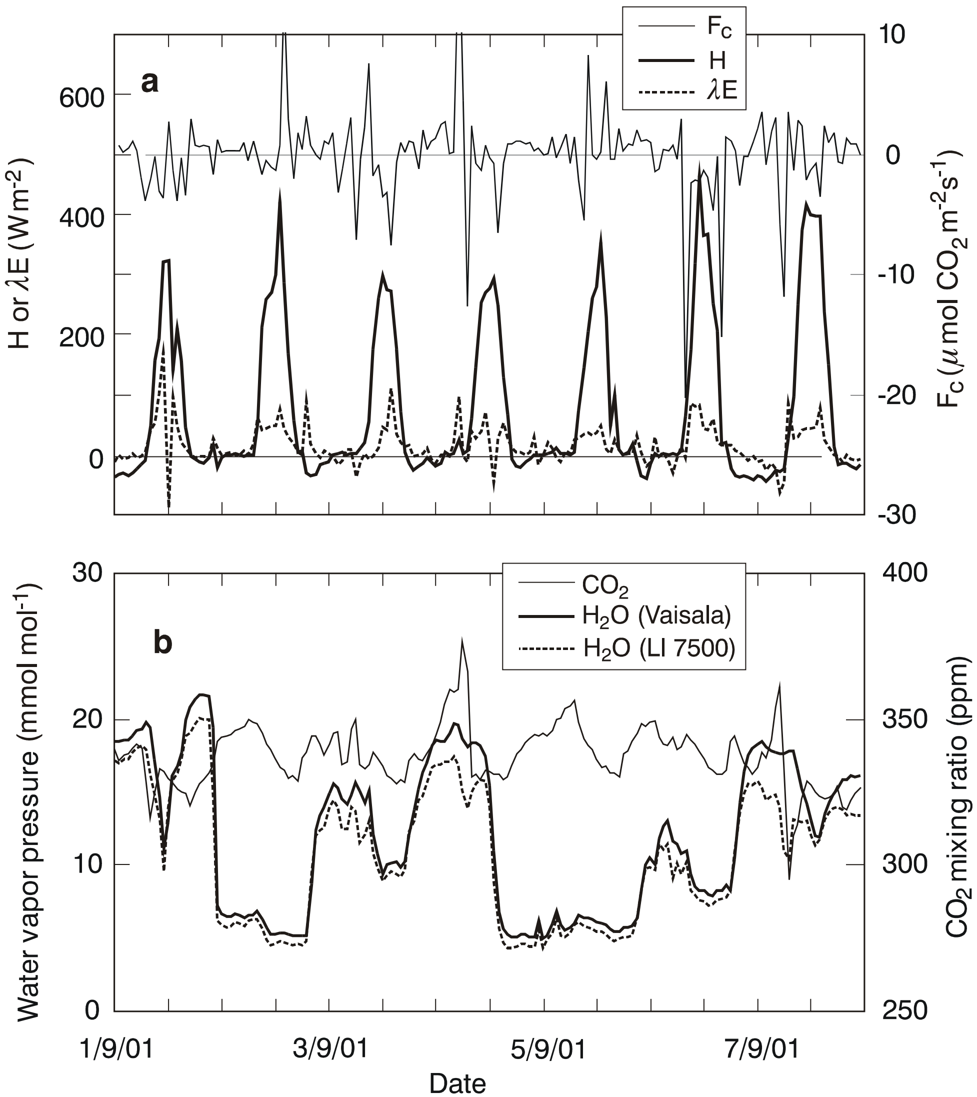

Figure 6. Time series of (a) the fluxes of H, λE and F_c and (b) CO_2 mixing ratio and water vapour pressure measured using a LI-7500 open-path infrared gas analyser and water vapour pressure from a Vaisala relative humidity sensor. Note the strong and rapid variations in humidity associated with synoptic weather fronts and with nocturnal boundary layer formation and dissipation.

Part 2: Results

- Meteorology
- Fluxes
- Water balances
- Annual budgets
- Comparison with international sites
- Extrapolation using MODIS data
- Revising MODIS algorithm

Some key drivers

Albedo

R_n - G

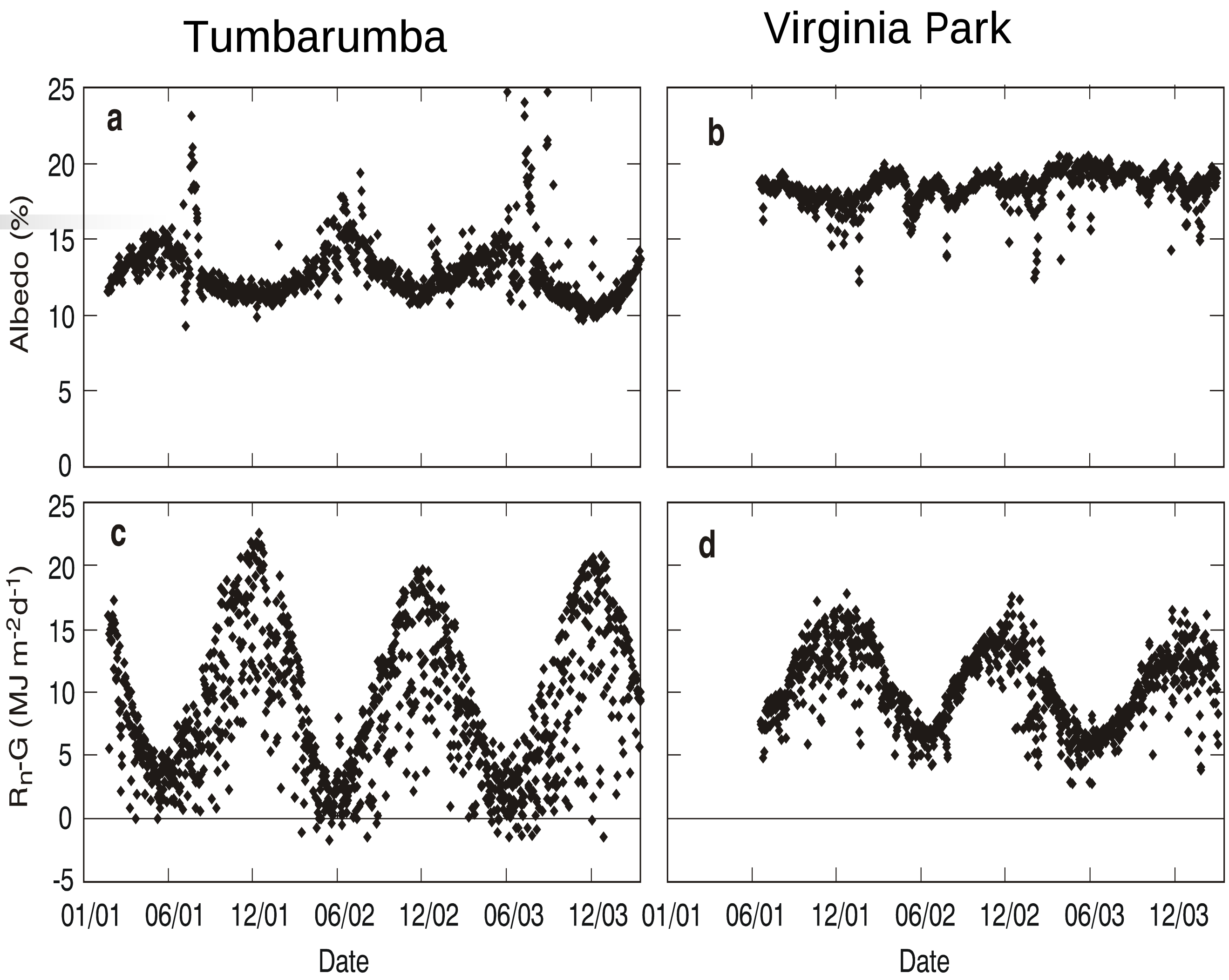

Figure 7. Daytime average albedo, α, and 24-hour averages of available energy, $R_n - G$, for Tumbarumba (a, c) and Virginia Park (b, d).

Humidity deficit
Temperature

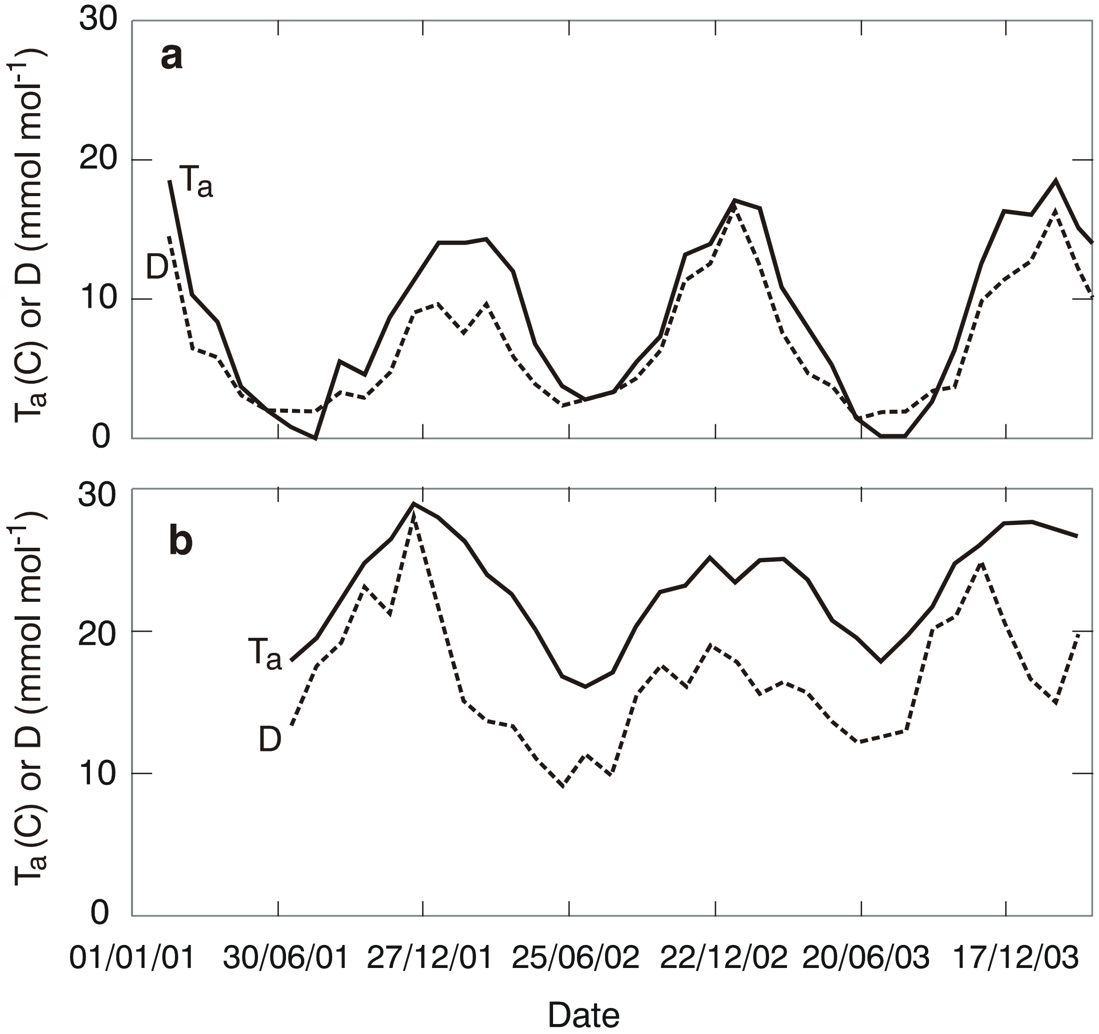

Figure 8. Monthly averages for daytime humidity deficit, *D*, and 24-hour mean air temperature, *T*a, for (a) Tumbarumba and (b) Virginia Park.

H_2O & CO_2 fluxes

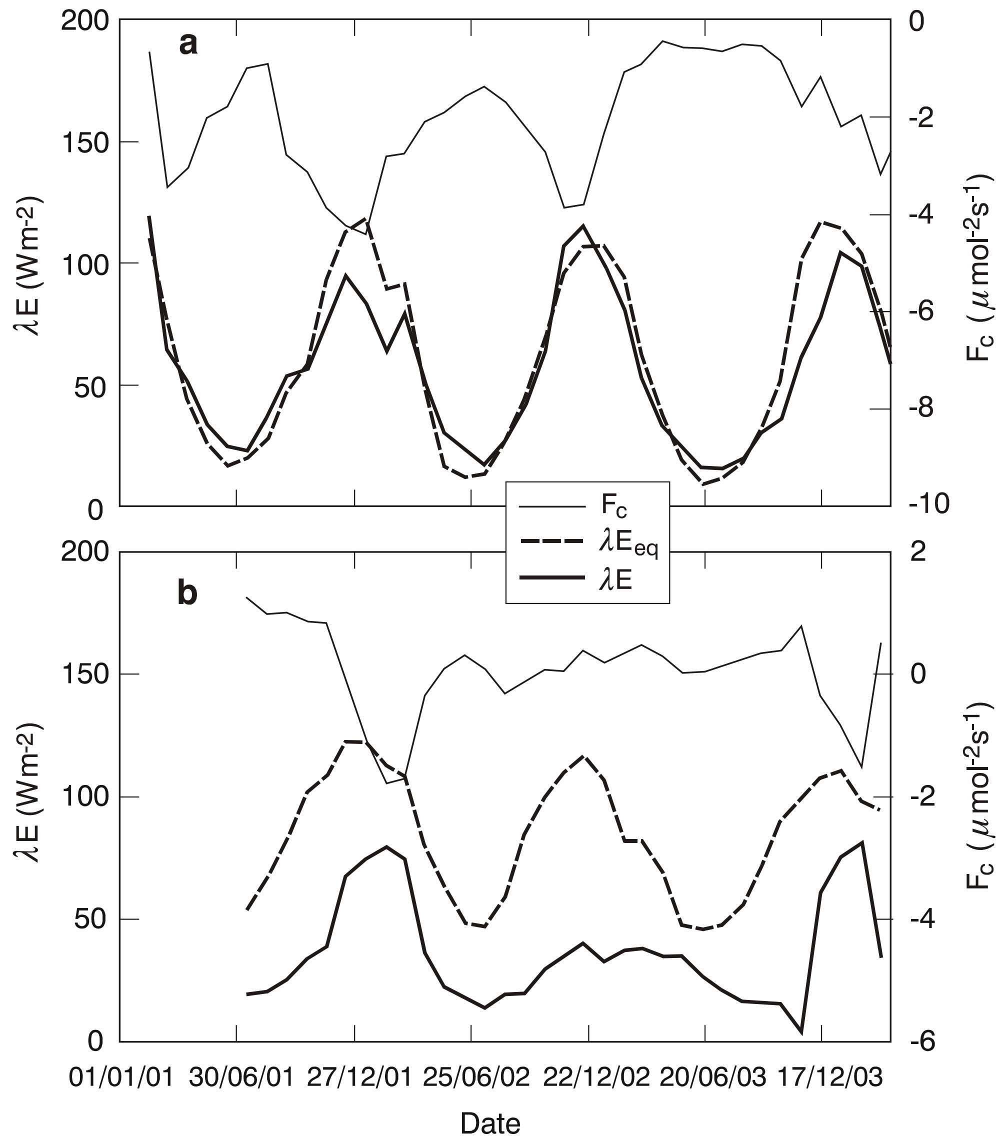

Figure 9. Monthly averages of the flux of CO2, *F*c, evapotranspiration, λ*E* and equilibrium evaporation, λ*E*eq for (a) Tumbarumba and (b) Virginia Park.

Water balances

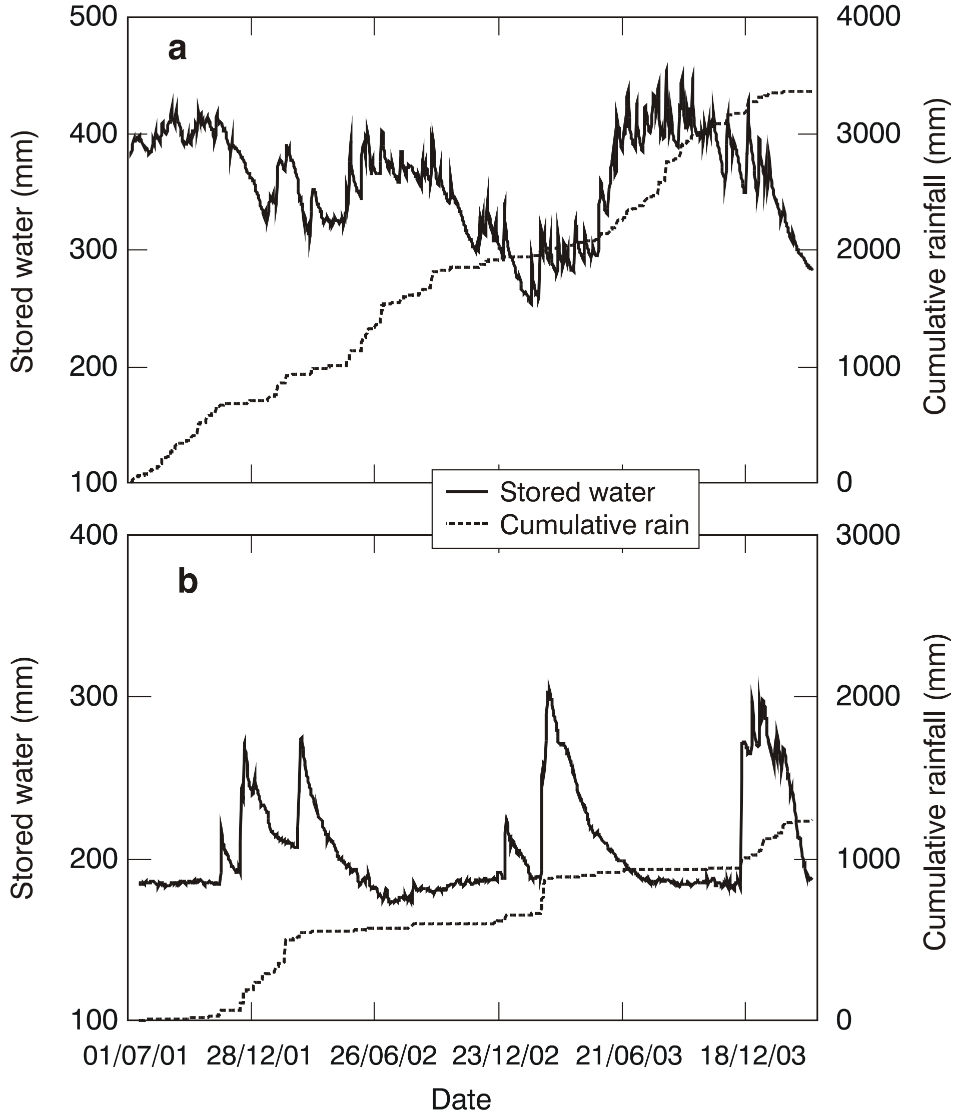

Figure 10. Water storage in the top 1.2 m of soil at Tumbarumba and cumulative rainfall from 1 July 2001. The contrast in rainfall patterns at the two sites is evident in the variation in soil moisture content.

Annual average fluxes

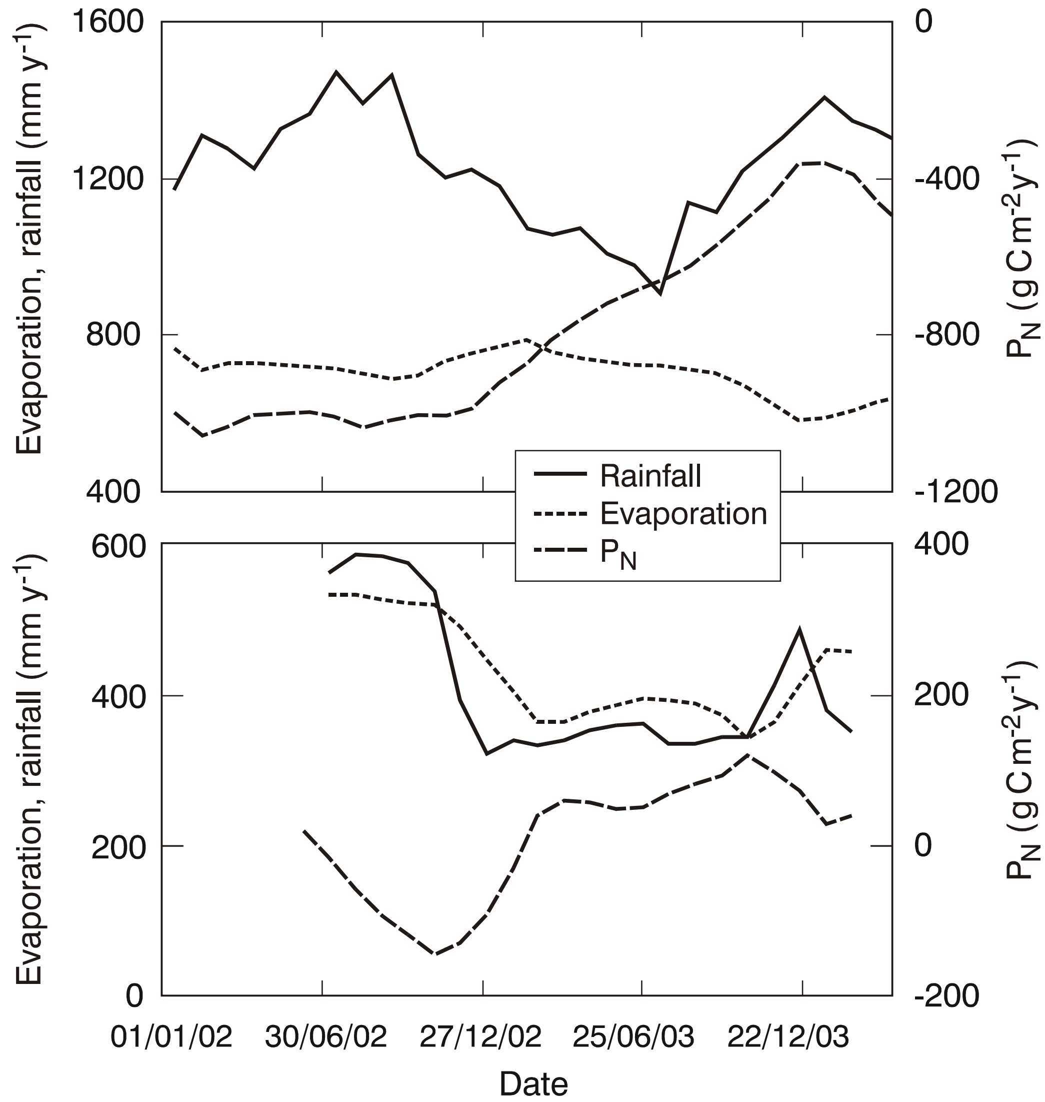

Figure 11. Twelve-month running totals for net ecosystem exchange of carbon, evapotranspiration and rainfall for (a) Tumbarumba and (b) Virginia Park. Reduction in annual productivity due to the 2002-03 drought is clearly evident.

Comparison with international sites

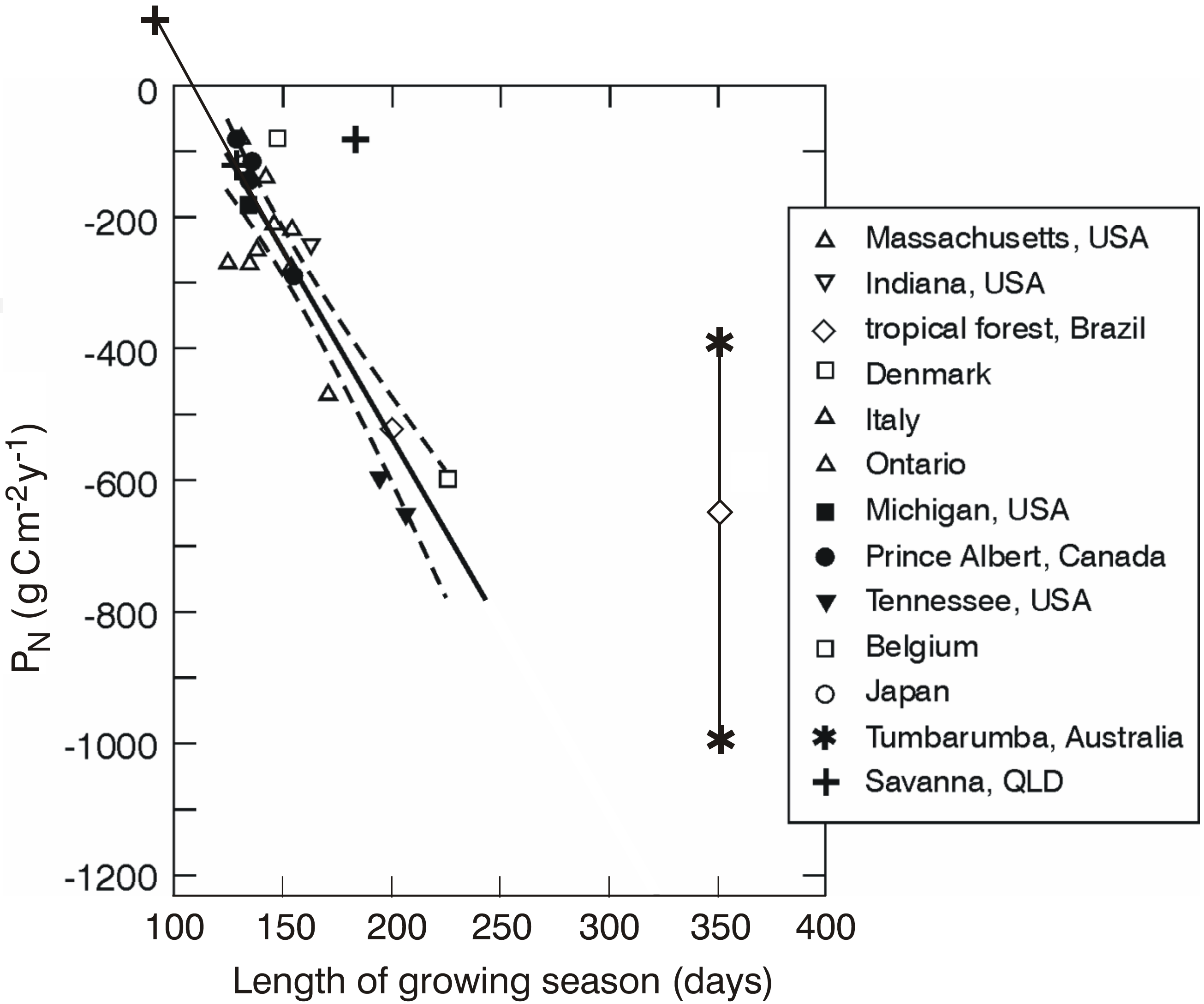

Figure 12. Net ecosystem exchange (NEE) measured at Tumbarumba and Virginia Park superimposed on data collated by Baldocchi et al (2001) for 11 international FLUXNET sites. *P*N is plotted as a function of length of growing season. Note the strong interannual variability at Tumbarumba.

MODIS LAI

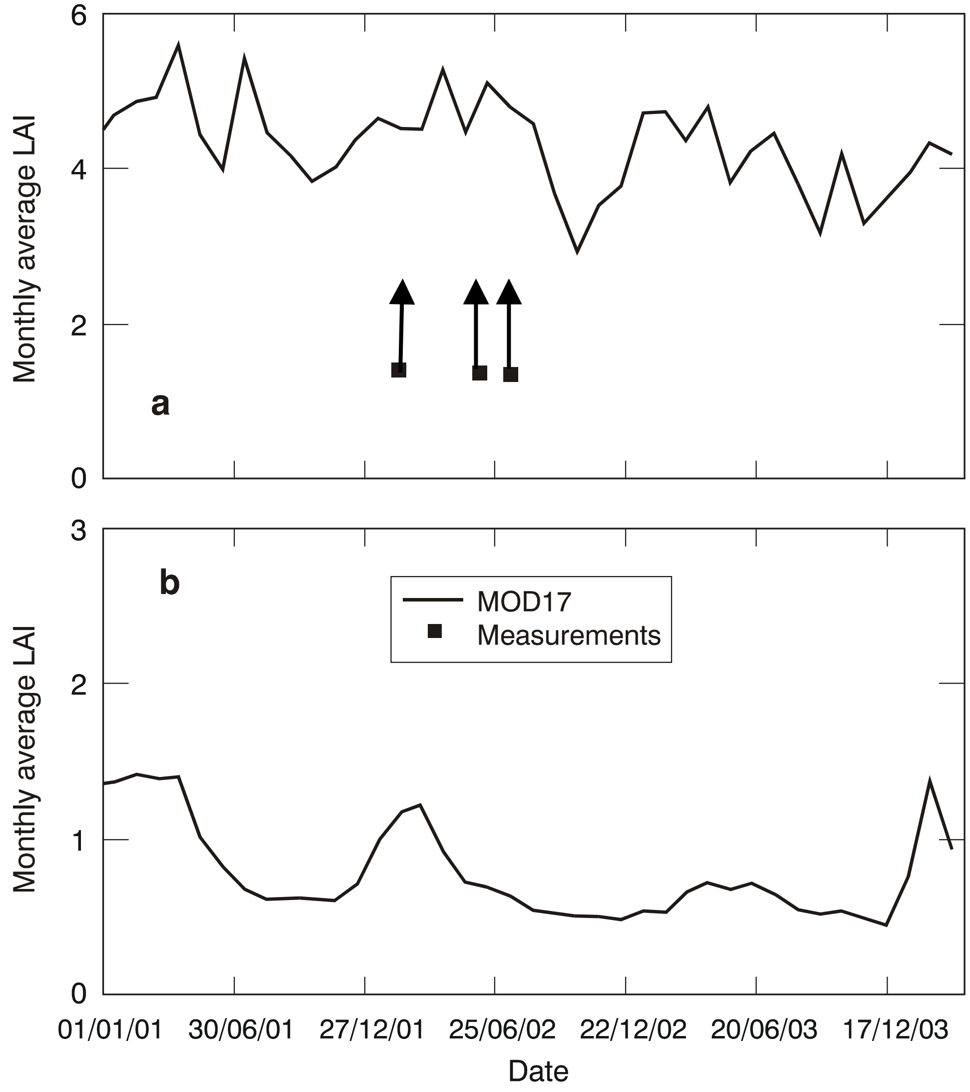

Figure 13. Estimates of mean monthly *L*ai from MOD17 for the 7 x 7 km areas surrounding (a) Tumbarumba and (b) Virginia Park flux stations. Also shown are estimates of *L*ai for the trees at Tumbarumba obtained using hemispherical photographs.

MODIS vs measured GPP

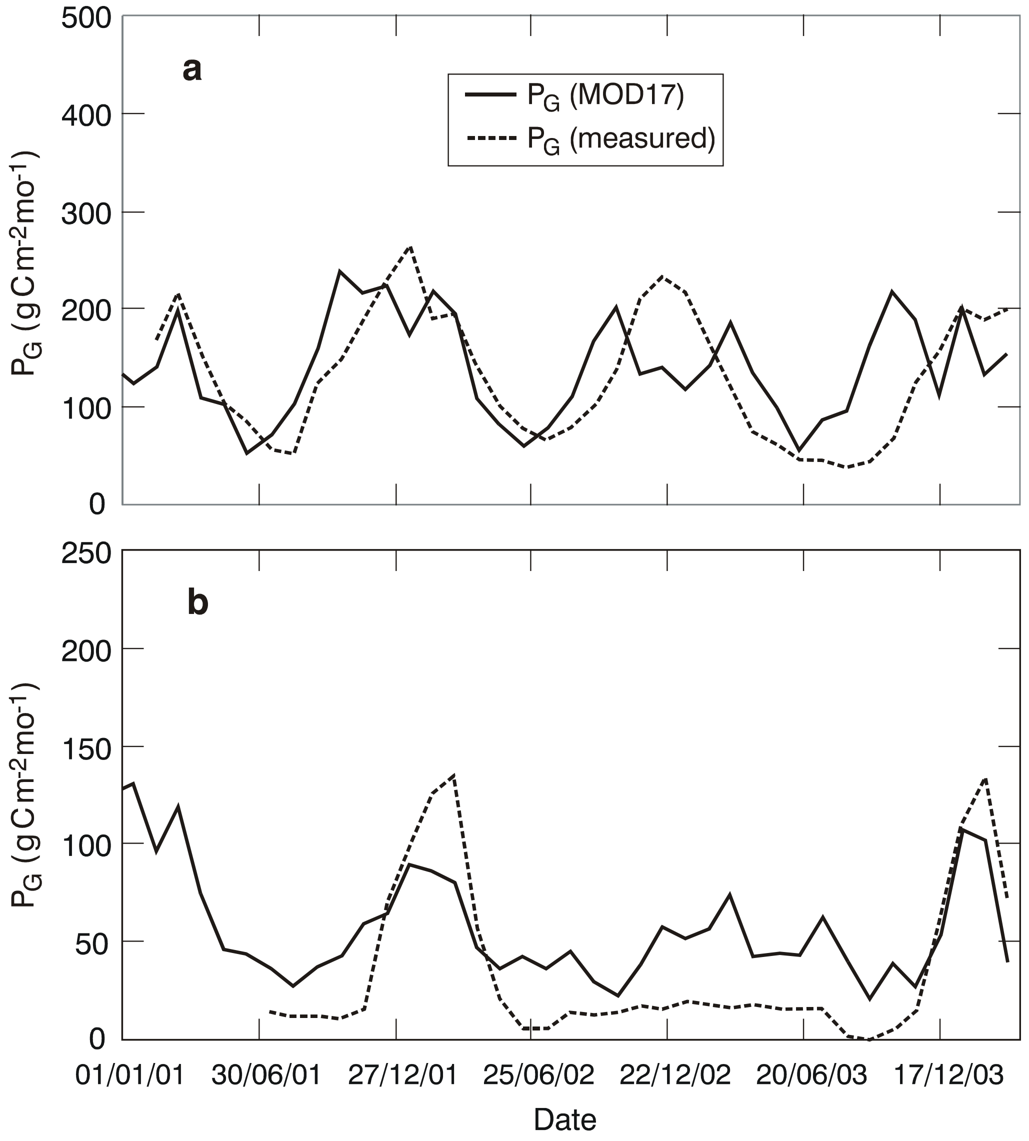

Figure 14. Monthly-averages for gross primary production, *P*G, predicted by the MOD17 algorithm and derived from flux measurements at (a) Tumbarumba and (b) Virginia Park. Note the difference in scale for the ordinate between the two figures.

MODIS GPP parameterization (1)

$$P_G = \alpha S_{abs} f(D) g(T)$$

$$f(D) = \begin{cases} 1, & D < D_{\min} \\ \dfrac{D_{\max} - D}{D_{\max} - D_{\min}}, & D_{\min} \le D \le D_{\max} \\ 0, & D > D_{\max} \end{cases}$$

$$g(T) = \begin{cases} 0, & T < T_{\min} \\ \dfrac{T_{\max} - T}{T_{\max} - T_{\min}}, & T_{\min} \le T \le T_{\max} \\ 1, & T > T_{\max} \end{cases}$$

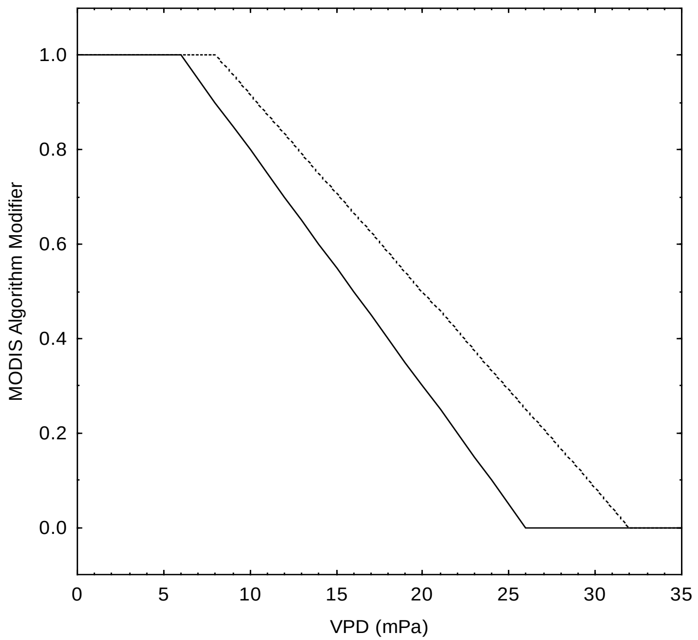

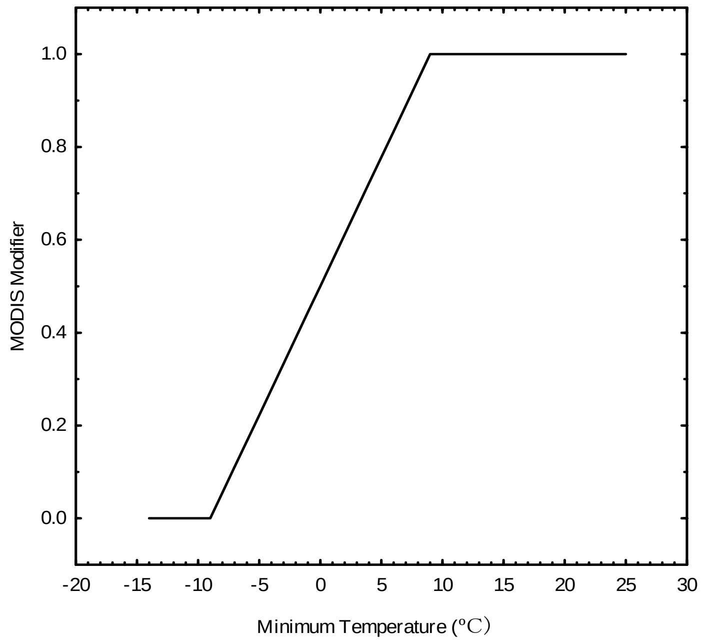

MODIS GPP parameterization (2)

$$P_G = \alpha S_{abs} f(D) g(T) h(X)$$

$$h(X) = \begin{cases} X, & X < 1 \\ 1, & X \geq 1 \end{cases}$$

$$X = \frac{\sum P}{\sum E} = \frac{a \sum P}{\sum \frac{s S_{abs}}{s + \gamma}}$$

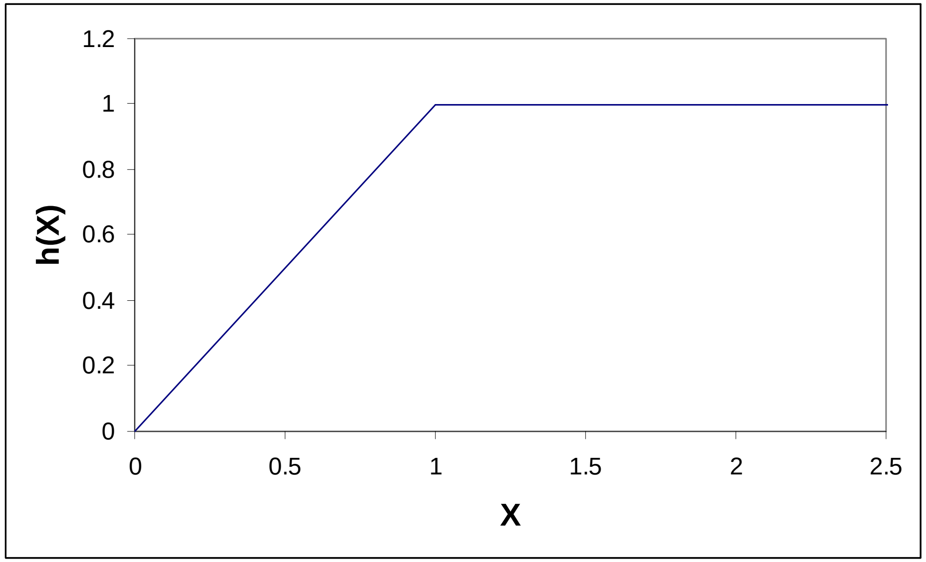

Original and modified MODIS GPP algorithms

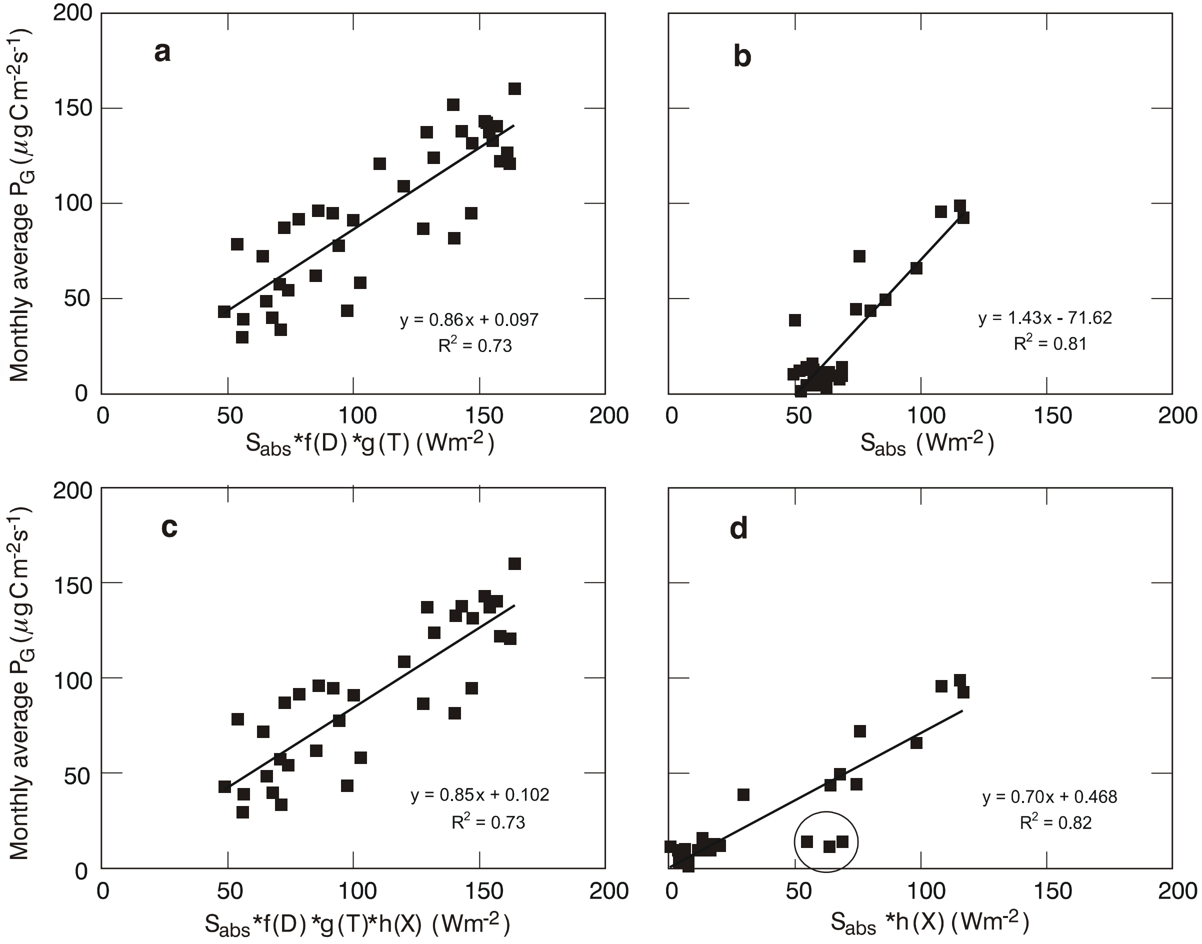

Figure 15. Monthly-averages for daytime P_G plotted as a function of (a) $S_{abs} f(D)g(T)$ for Tumbarumba and (b) at Virginia Park. Modifications to the MOD17 algorithm to include the soil moisture availability index $h(X)$ (Equation 11) are shown in (c) for Tumbarumba and in (d) for Virginia Park. The main effect is to reduce the effective radiation use efficiency from 1.43 to 0.70 g C MJ^{-1} PAR and to lower the light compensation point from 50 to 0 W m^{-2} at Virginia Park. There is little change in the linear regression for Tumbarumba. The three circled points correspond to the low-rainfall wet season of 2002-03.

Revised MODIS GPP time series

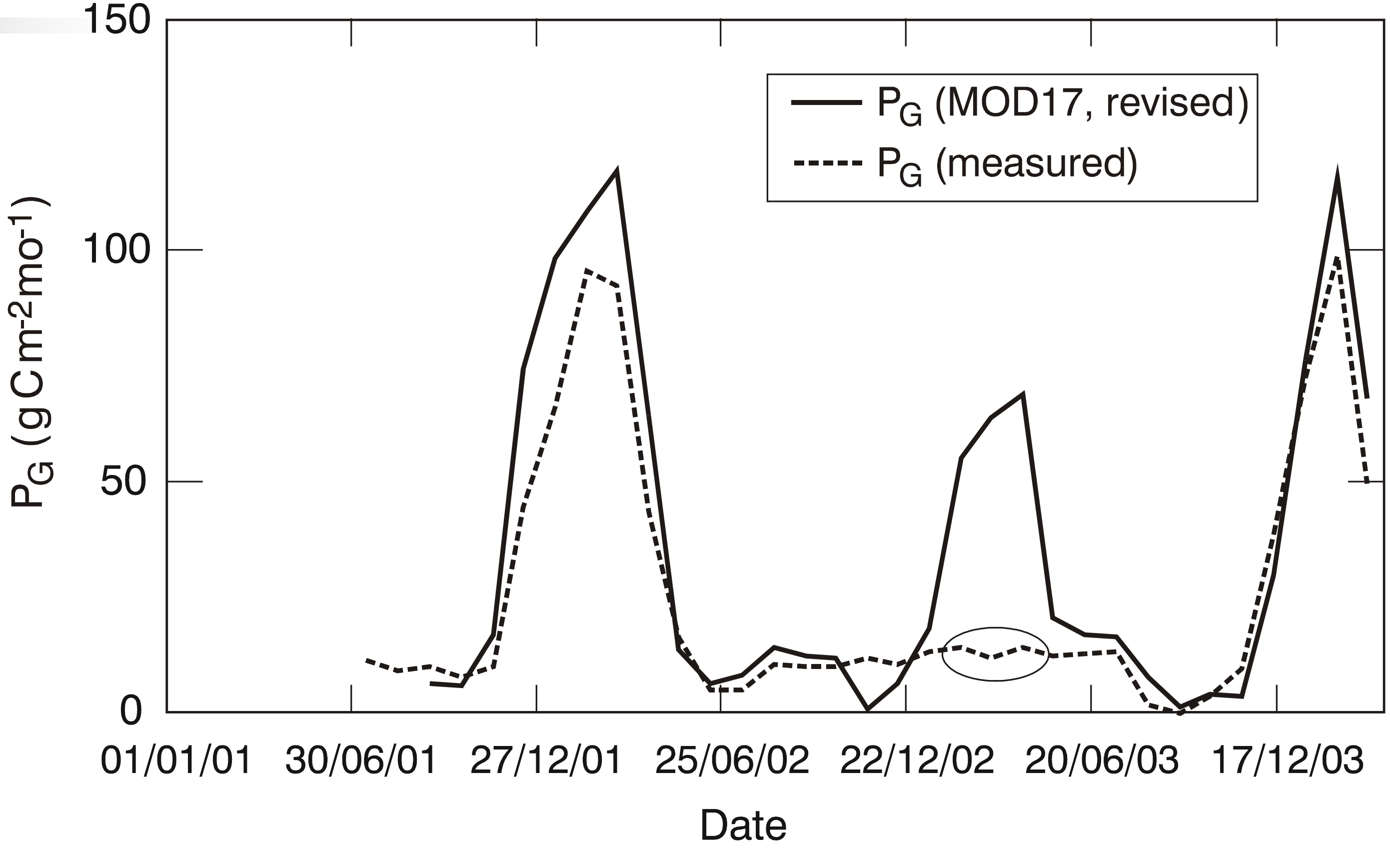

Figure 16. Monthly-averages for gross primary production, P_G, at Virginia Park derived from flux measurements and from the modified algorithm (Equation 11). The three circled points correspond to the low-rainfall wet season of 2002-03.